Supporting Information

Engineering Molecular Heterojunctions in 2D MOFs for Efficient Charge Separation and CO_2 Photoreduction

Yan Rong[a], Xinqi Pan[a], Xi Wang[b], Shanshan Zheng[a], Zhifeng Xina*[a], Shang-Bing Wang[a], Zhaoxu Wang*[c]

[a] Institute of Molecular Engineering and Applied Chemistry, Anhui University of Technology, Ma'anshan, Anhui 243002, P. R. China.
E-mail: xinzf521@ahut.edu.cn
[b] School of Chemistry and Chemical Engineering, Anhui University of Technology, Ma'anshan, Anhui 243002, P. R. China.
[c] School of Chemistry and Chemical Engineering, Hunan University of Science and Technology, Xiangtan 411201, P. R. China, E-mail: hnust_chem@163.com.
E-mail: hnust_chem@163.com

Experimental section

Materials

All chemicals were obtained from commercial sources and used as received. Copper(II) acetate monohydrate ($Cu(CH_3COO)_2 \cdot H_2O$), 2,3,6,7,10,11-hexahydroxytriphenylene (HHTP), N,N-dimethylformamide (DMF), zinc nitrate hexahydrate ($Zn(NO_3)_2 \cdot 6H_2O$), methanol (CH_3OH), triethanolamine (TEOA), sodium sulfate (Na_2SO_4), and Nafion solution were purchased from Sinopharm Chemical Reagent Co., Ltd. 5,10,15,20-tetrakis[4-(1H-imidazol-1-yl)phenyl]porphyrin was supplied by Jinan Henghua Chemical Technology Co., Ltd. Deionized water was produced using a Qingdao Fulham ultrapure water system. ^{13}C-labeled CO_2 (99 atom % ^{13}C) was obtained from Cambridge Isotope Laboratories.

Syntheses of Samples

Synthesis of Zn-TIPP: 30 mg $Zn(NO_3)_2 \cdot 6H_2O$ was dissolved in 28 mL DMF and 2 mL ultrapure water and sonicated for thirty minutes. In another baker, 12 mg of TIPP was dissolved in 5 mL of CH_3OH and sonicated for 20 minutes. The two solutions were

mixed and stirred for 24 hours. A purplish-red powder was collected by filtration and washed with water and acetone for three times, respectively, and then dried at 60°C under vacuum for 12 hours.

Synthesis of Cu-HHTP: 32.4 mg of HHTP and 10.5 mg of Cu $(Ac)_2 \cdot H_2O$ were dissolved in 2.5 mL of DMF and 2.5 mL of water and sonicated for 15 minutes, and then the mixture was heated to 85 °C for 12 hours. After cooling to room temperature, the dark blue powder was collected by filtration, washed with water and methanol for three times, respectively, and then dried at 60 °C under vacuum for 12 hours.

Synthesis of Zn-TIPP+Cu-HHTP: 45 mg of Cu-HHTP and 5 mg of Zn-TIPP were added to the agate mortar and ground for 30 minutes. A dark purple powder was obtained.

Synthesis of Zn-TIPP/Cu-HHTP: Initially, Cu-HHTP nanosheets (20 mg) were dispersed in DMF (30 mL) and subjected to ultrasonication (180 W) for 4 h. Subsequently, Zn $(NO_3)_2 \cdot 6H_2O$ (30 mg) was added to the dispersion under continuous stirring for 20 min. A pre-prepared ligand solution of TIPP (12 mg in 5 mL methanol) was then introduced dropwise into the mixture. After additional stirring for 20 min, the suspension was sealed and sonicated (200 W) for 6 h. The resulting green precipitate was collected by centrifugation, washed repeatedly with water and acetone (three times each), and dried under vacuum at 60 °C overnight to obtain the Zn-TIPP/Cu-HHTP composite. In addition, Zn-TIPP/Cu-HHTP composites with different loadings were prepared by varying the amount of Zn $(NO_3)_2 \cdot 6H_2O$ (15 mg and 45 mg).

Synthesis of Zn-TIPP/b-Cu-HHTP:

The preparation method is like that of Zn-TIPP/Cu-HHTP, except that Cu-HHTP is used directly without prior exfoliation.

Photocatalytic CO_2RR

The photocatalytic CO_2 reduction procedure is as follows: First, 5 mg of Zn-TIPP/Cu-HHTP is dispersed in 30 mL of deionized water and treated with 200 W ultrasound for 30 minutes. The resulting dispersion is then transferred to a 100 mL photoreactor. To

remove dissolved air, the reactor is purged with CO_2 (1 atm) for 30 minutes before being sealed. The reaction was carried out under continuous stirring and irradiation from a 300 W xenon lamp fitted with a 420 nm cutoff filter. Formic acid production was quantified at two-hour intervals by ion chromatography (IC), and the product identity was confirmed by ^1H NMR spectroscopy.

Photoelectrochemical measurements

Photoelectrochemical measurements were conducted using a CHI660E electrochemical workstation equipped with a standard three-electrode configuration. A modified indium-tin oxide (ITO) glass slide served as the working electrode, while an Ag/AgCl electrode and a carbon rod were used as the reference and counter electrodes, respectively. The measurements were performed in a 0.2 M Na_2SO_4 aqueous electrolyte. Mott–Schottky plots were obtained at alternating frequencies of 1500, 2000, and 2500 Hz. Transient photocurrent responses were recorded over ten on-off cycles of visible-light irradiation (20 s per interval). Electrochemical impedance spectroscopy (EIS) was carried out in the frequency range of 0.1 Hz to 10 MHz.

For the working electrode preparation, Zn-TIPP-Cu-HHTP (2 mg) was dispersed in a mixture of ethanol (900 μL) and 0.1 wt% Nafion solution (100 μL) and sonicated for 25 min. A 200 μL aliquot of the resulting suspension was drop-cast onto a pre-cleaned ITO substrate (active area = 1 cm^2) and dried at 55 °C to form a uniform catalyst film.

Carbon isotope tracer measurements

5 mg of Zn-TIPP/Cu-HHTP was dispersed in 30 mL of ultrapure deionized water in an 80-millilitre reactor and bubbled with high purity Ar for 30 min to remove residual air. Subsequently, $^{13}CO_2$ was introduced into the reaction system. Photocatalytic reaction experiments were carried out according to the same methodology and the photocatalytic products were detected using nuclear magnetic resonance (NMR).

NMR measurements

The liquid product was analyzed by nuclear magnetic resonance (NMR) spectroscopy using deuterated dimethyl sulfoxide (DMSO-d_6) as the solvent. For sample preparation,

400 μL of the reaction solution was combined with 100 μL of DMSO-d_6 in an NMR tube prior to measurement.

Characterizations

Powder X-ray diffraction (PXRD) patterns were collected on a Bruker D8 Advance diffractometer equipped with Cu Kα radiation (λ = 1.5406 Å, Ni-filtered) at 40 kV and 20 mA, using a scan rate of 5° min^{-1}. Transmission electron microscopy (TEM) and energy-dispersive X-ray spectroscopy (EDXS) were performed on a JEOL JEM-2100 microscope operated at 200 kV for morphological and elemental mapping analysis. Nitrogen and carbon dioxide adsorption–desorption isotherms were recorded on a Micromeritics ASAP 2460 analyzer; all samples were degassed under vacuum at 100 °C for 8 h prior to analysis. Thermogravimetric analysis (TGA) was carried out using a Shimadzu DTG-60H thermal analyzer. Fourier-transform infrared (FT-IR) spectra were obtained with a Nicolet 6700 spectrometer. Solid-state UV-vis diffuse reflectance spectra (UV-vis DRS) were acquired on a Shimadzu UV-3600 spectrophotometer. Photoluminescence (PL) spectra were measured on an Edinburgh FLS980 fluorescence spectrometer. ^{1}H nuclear magnetic resonance (NMR) spectra were recorded on a Bruker AVANCE 400 Plus spectrometer (400 MHz) with DMSO-d_6 as the solvent. Ion chromatography (IC) analysis was conducted on a Shimadzu LC20ADsp system. Gas chromatography (GC) was performed using a Shimadzu GC-2010 Plus instrument equipped with a flame ionization detector. Photochemical experiments employed a 300 W Xe lamp (CEC Jinyuan, F300) as the light source. Ultrasonic treatment was performed using a cell disruptor (Ningbo Xinzhi Biotechnology Co., Ltd.).

Computational details

All density functional theory (DFT) calculations were performed with the Vienna Ab Initio Simulation Package (VASP)[1–3]. The exchange–correlation functional was treated within the generalized gradient approximation (GGA) using the revised Perdew–Burke–Ernzerhof (rPBE) functional[4]. The projector-augmented wave (PAW) method[5,6] was employed to describe core electrons, and valence wave functions were expanded in a plane-wave basis set with a kinetic energy cutoff of 420 eV. Geometry

optimizations were considered converged when the total energy change between successive steps fell below 10–5 eV and the Hellmann–Feynman forces on all relaxed atoms were less than 0.02 eV $Å^{-1}$.

The Gibbs free energy change (ΔG) for each elementary step of the CO_2 reduction reaction (CO_2RR) involving proton–electron transfer was evaluated using the computational hydrogen electrode (CHE) model[7,8]. At the standard potential (U = 0 V vs. RHE), ΔG was computed as:

$$\Delta G = \Delta E + \Delta EZPE - T\Delta S + \int CP\, dT$$

where ΔE is the DFT-derived electronic energy difference between product and reactant states; ΔEZPE and ΔS represent the zero-point energy and entropy corrections, respectively, obtained from vibrational frequency calculations at 298.15 K; and the integral term accounts for the enthalpy correction due to heat capacity.

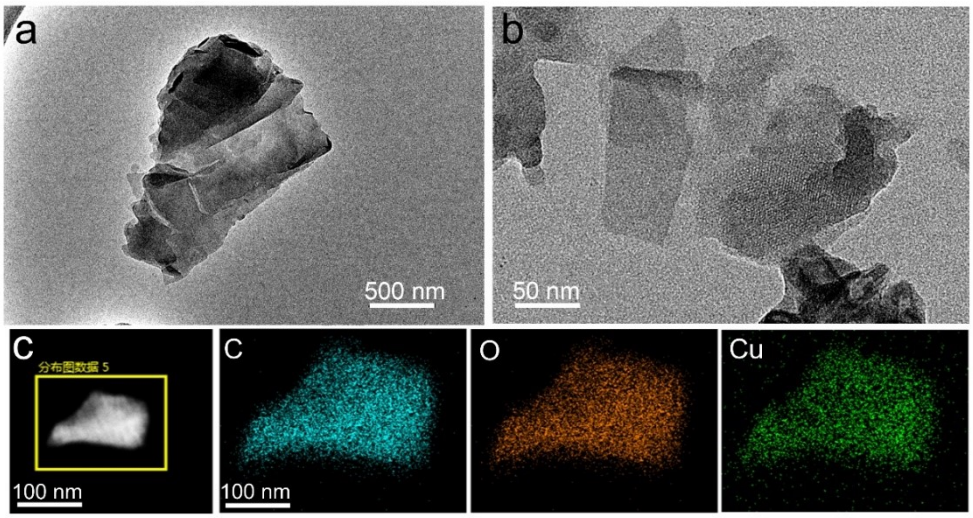

Fig S1. Characterizations of Cu-HHTP. (a) TEM image. (b) HRTEM image. (c) STEM and EDS elemental mapping.

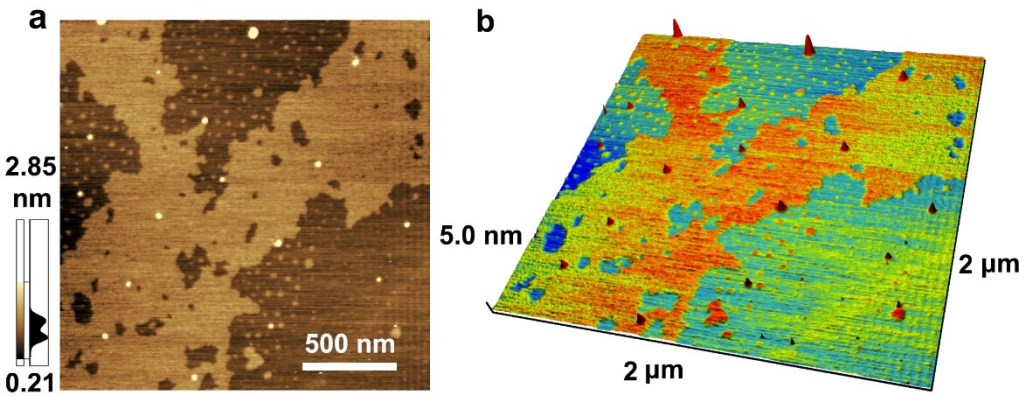

Fig S2. AFM images of Zn-TIPP/Cu-HHTP. (a) AFM image. (b) 3D mode image.

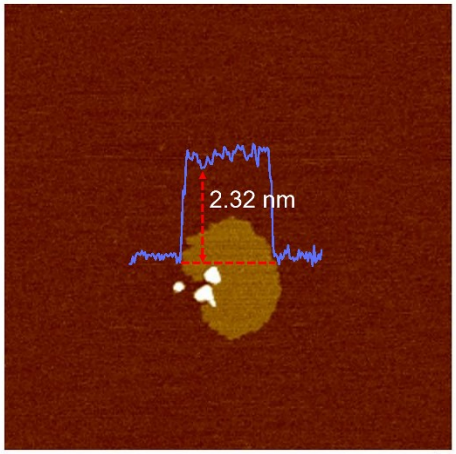

Fig S3. AFM images of Cu-HHTP.

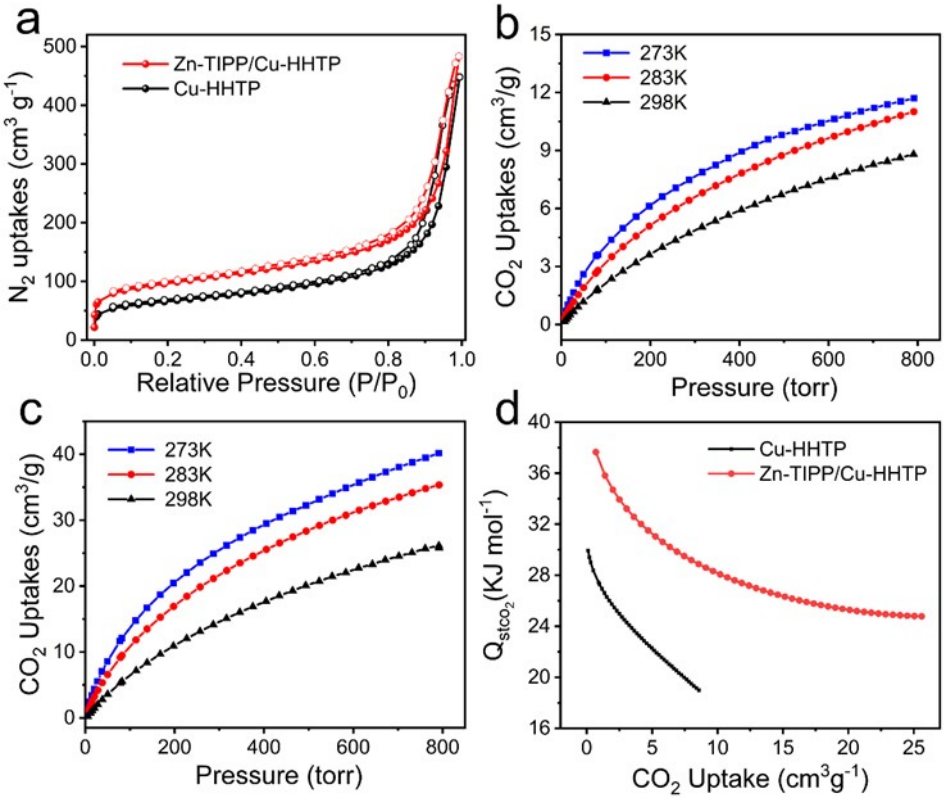

Fig S4. Gases adsorption performance of Cu-HHTP and Zn-TIPP/Cu-HHTP. (a) N_2 sorption isotherms at 77 K. (b) CO_2 adsorption curves of Cu-HHTP at different temperatures. (c) CO_2 adsorption curves of Zn-TIPP/Cu-HHTP at different temperatures. (d) CO_2 adsorption enthalpy of Cu-HHTP and Zn-TIPP/Cu-HHTP.

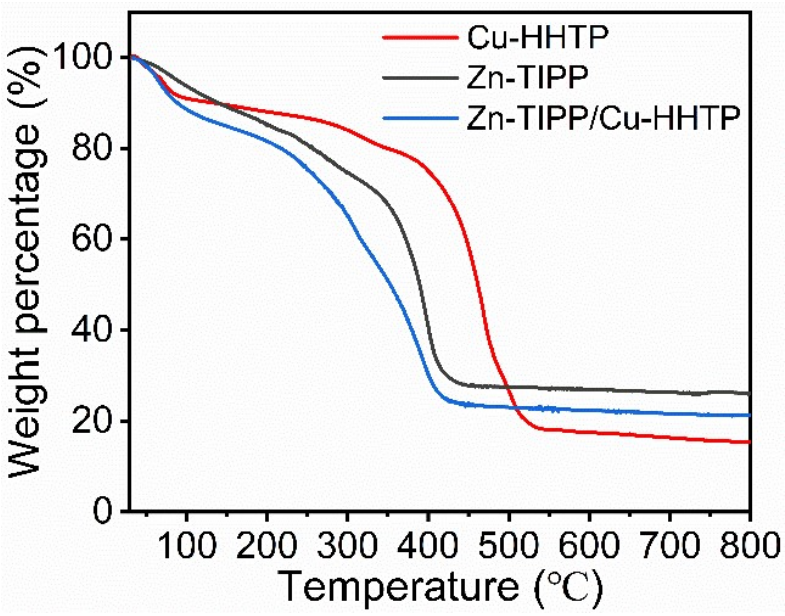

Fig S5. TGA measurement of Zn-TIPP, Cu-HHTP and Zn-TIPP/Cu-HHTP.

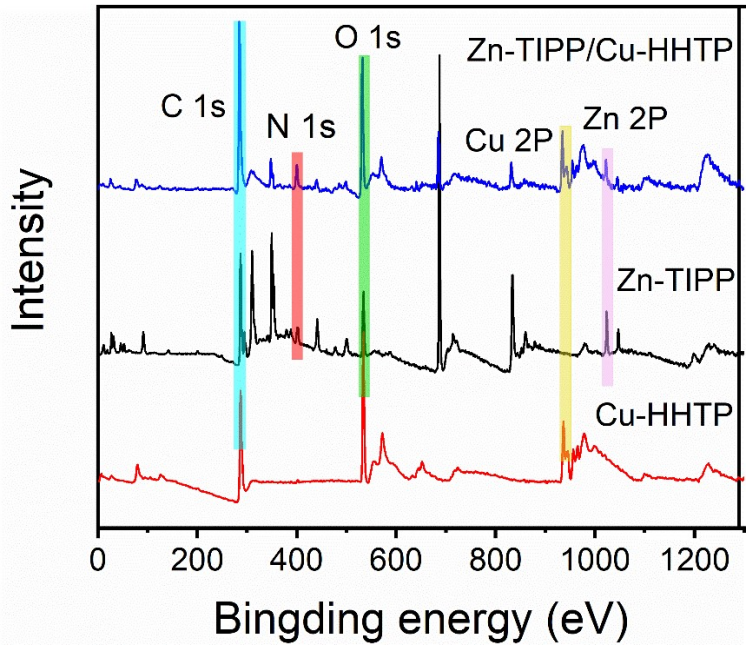

Fig S6. Total XPS spectra of Zn-TIPP, Cu-HHTP and Zn-TIPP/Cu-HHTP.

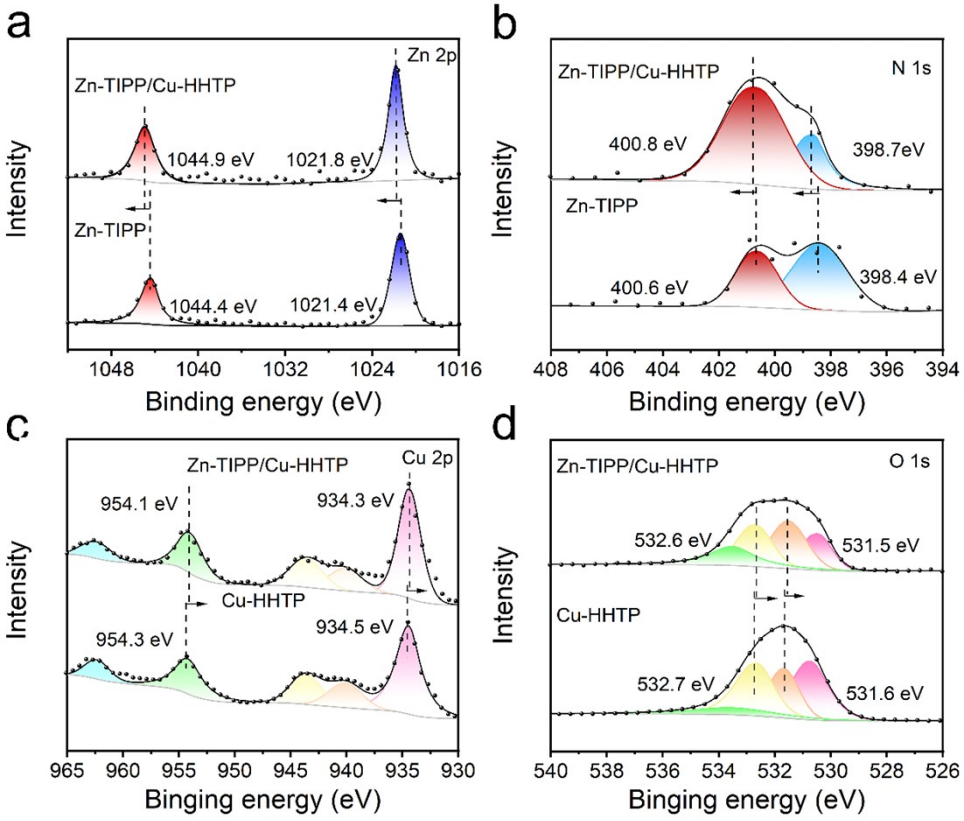

Fig S7. XPS spectra of Zn-TIPP, Cu-HHTP and Zn-TIPP/Cu-HHTP. (a) Zn 2p. (b) N 1s. (c) Cu 2p. (d) O 1s.

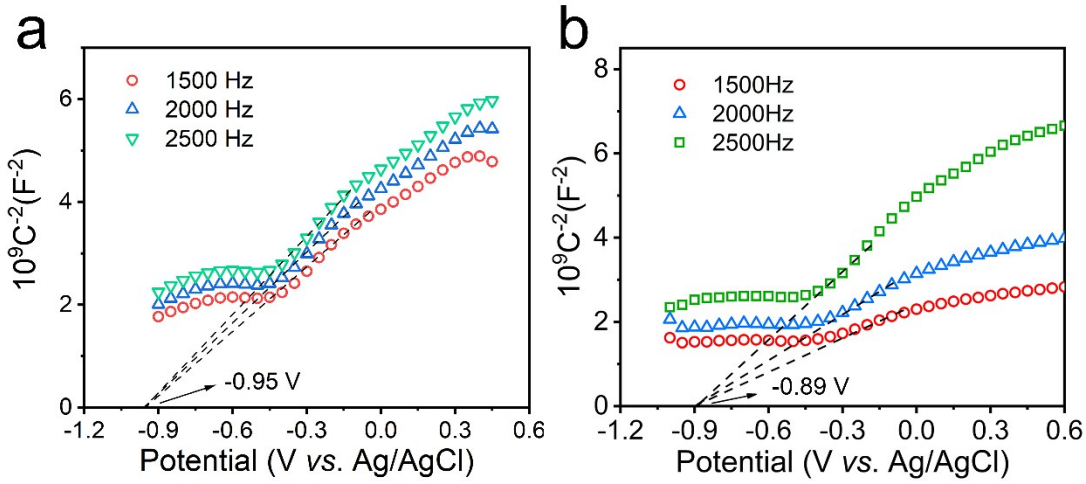

Fig S8. Mott–Schottky plots of different samples. (a) Zn-TIPP, (b) Cu-HHTP.

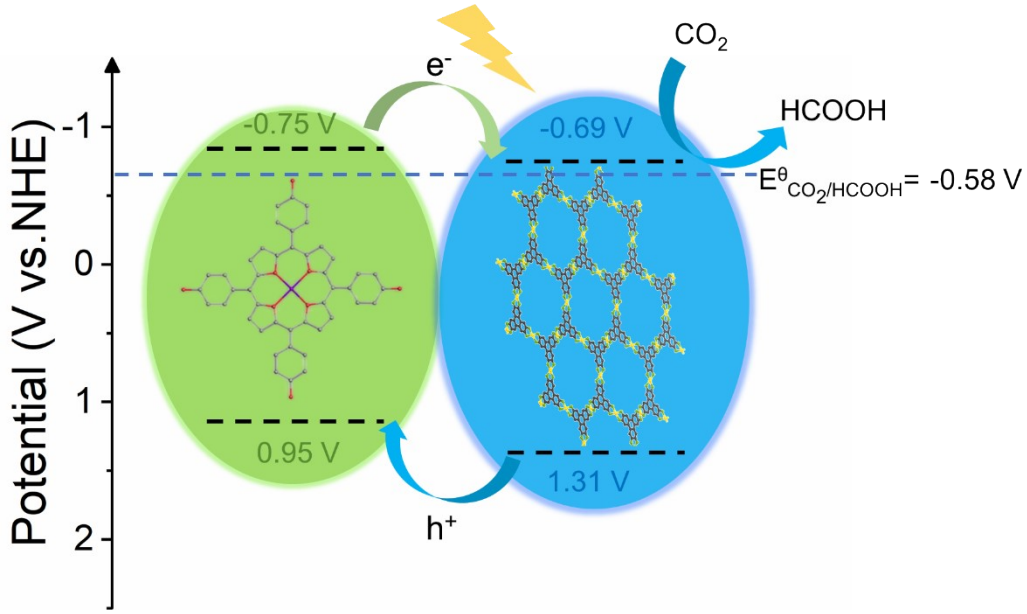

Fig S9. Energy band structure diagram of Zn-TIPP/Cu-HHTP during CO_2 photoreduction.

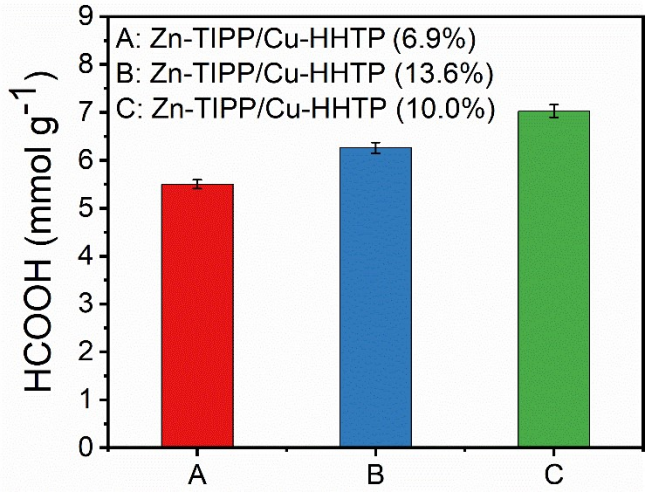

Fig S10. Comparison of Formic Acid Production Performance with Different Loadings.

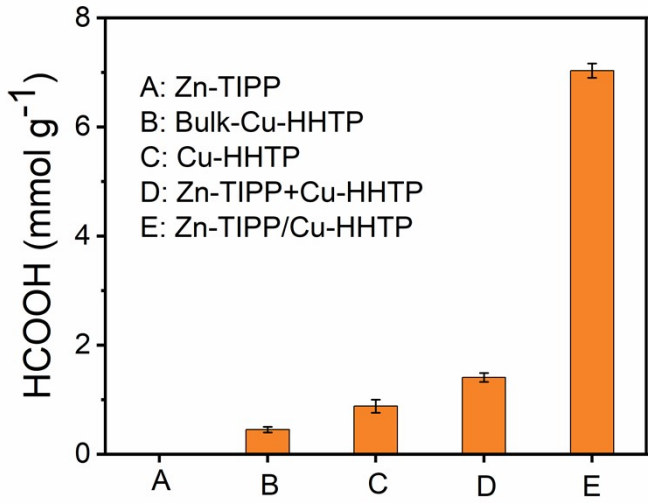

Fig S11. The yield of HCOOH after 10 h of reaction over different catalysts.

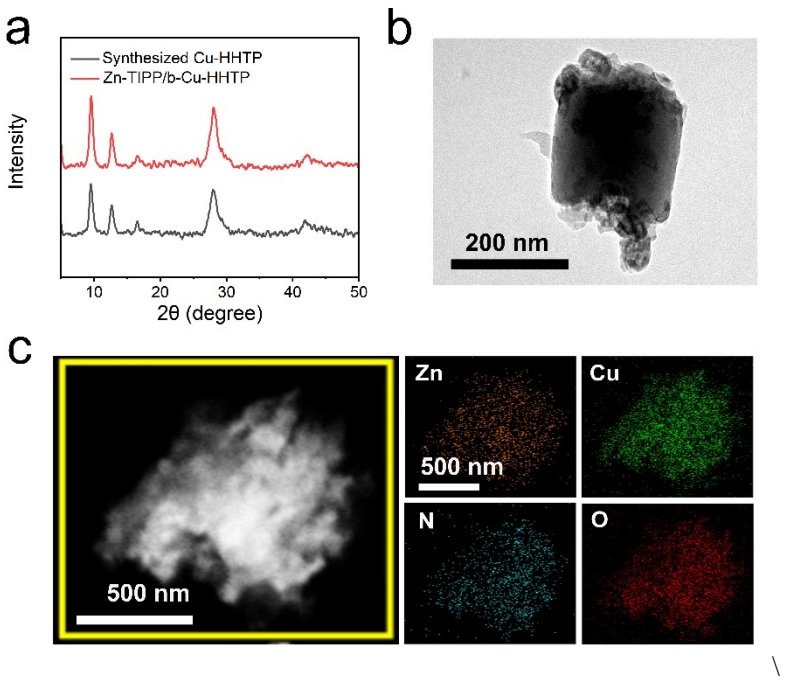

Fig S12. Characterization of Zn-TIPP/b-Cu-HHTP. (a) PXRD patterns. (b) TEM spectra of Zn-TIPP/b-Cu-HHTP. (c) STEM and elemental mapping images of Zn-TIPP/b-Cu-HHTP.

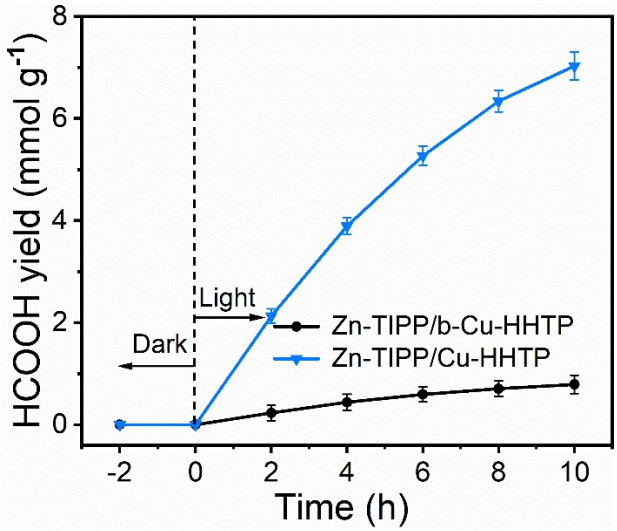

Fig S13. HCOOH yields of Zn-TIPP/Cu-HHTP and Zn-TIPP/b-Cu-HHTP at different times.

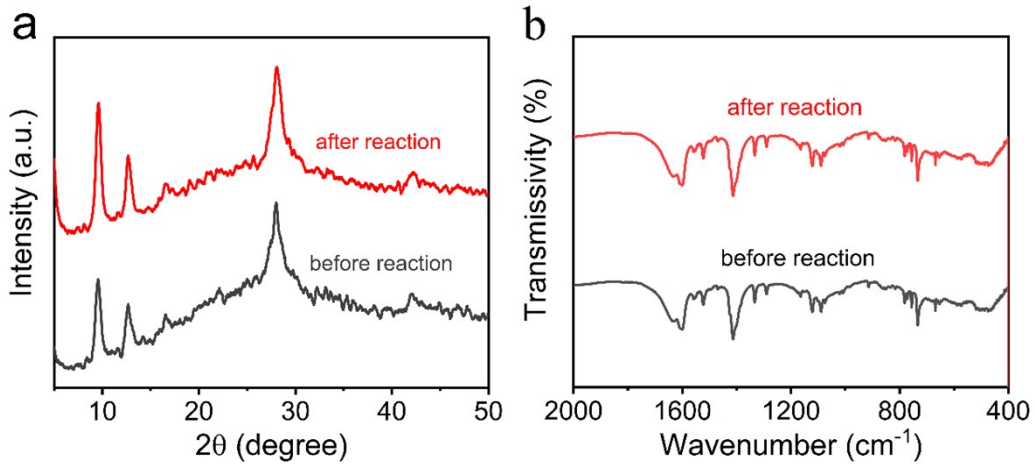

Fig S14. PXRD and FTIR Characterization of Zn-TIPP/Cu-HHTP before and after photocatalytic reaction. (a) PXRD patterns. (b) FTIR spectra.

Table S1. Elemental Ratio in Zn-TIPP/Cu-HHTP.

	ICP-OES (wt%)	
Sample	Cu	Zn
Zn-TIPP/Cu-HHTP (6.9%)	7.36	0.48
Zn-TIPP/Cu-HHTP (10.0%)	7.11	0.69
Zn-TIPP/Cu-HHTP (13.6%)	6.79	0.94

Reference

[1] G. Kresse, J. Hafner, *Phys. Rev. B* 1993, **48**, 13115.
[2] G. Kresse, J. Furthmüller, *Phys. Rev. B* 1996, **54**, 11169.
[3] J. P. Perdew, K. Burke, M. Ernzerhof, *Phys. Rev. Lett.* 1996, **77**, 3865.
[4] P. E. Blöchl, *Phys. Rev. B* 1994, **50**, 17953.
[5] K. Mathew, V. S. C. Kolluru, S. Mula, S. N. Steinmann, R. G. Hennig, *The Journal of Chemical Physics* 2019, **151**, 234101.
[6] K. Mathew, R. Sundararaman, K. Letchworth-Weaver, T. A. Arias, R. G. Hennig, *The Journal of Chemical Physics* 2014, **140**, 084106.
[7] G.-R. Zhang, S. Wöllner, *Applied Catalysis B: Environmental* 2018, **222***,* 26.
[8] T. Luo, J. Zhang, W. Li, Z. He, X. Sun, J. Shi, D. Shao, B. Zhang, X. Tan, B. Han, *ACS Appl. Mater. Interfaces* 2017, **9**, 41594